

Mechanism of Carbamate Inactivation of FAAH: Implications for the Design of Covalent Inhibitors and In Vivo Functional Probes for Enzymes

Jessica P. Alexander and Benjamin F. Cravatt*

The Skaggs Institute for Chemical Biology and
Departments of Cell Biology and Chemistry
The Scripps Research Institute
10550 North Torrey Pines Road
La Jolla, California 92037

Summary

Fatty acid amide hydrolase (FAAH) regulates a large class of signaling lipids, including the endocannabinoid anandamide. Carbamate inhibitors of FAAH display analgesic and anxiolytic properties in rodents. However, the mechanism by which carbamates inhibit FAAH remains obscure. Here, we provide biochemical evidence that carbamates covalently modify the active site of FAAH by adopting an orientation opposite of that originally predicted from modeling. Based on these results, a series of carbamates was designed that display enhanced potency. One agent was converted into a “click chemistry” probe to comprehensively evaluate the proteome reactivity of FAAH-directed carbamates in vivo. These inhibitors were selective for FAAH in the nervous system, but they reacted with several enzymes in peripheral tissues. The experimental strategy described herein can be used to create in vivo probes for any enzyme susceptible to covalent inhibition.

Introduction

A wide range of lipids serve as endogenous signaling molecules in both the nervous system and periphery, including prostaglandins [1], lysophospholipids [2], and fatty acids and their derivatives [3, 4]. One class of lipid transmitters, the fatty acid amides [3, 4], has been shown to modulate a number of physiological and behavioral processes, such as pain [5], feeding [6], and sleep [7]. Representative fatty acid amides (FAAs) include the endogenous cannabinoid *N*-arachidonoyl ethanolamine (anandamide) [8], the anti-inflammatory lipid *N*-palmitoyl ethanolamine (PEA) [9], and the sleep-inducing substance 9(*Z*)-octadecenamide (oleamide) [7]. In contrast to aqueous-soluble chemical transmitters, which can be sequestered within membrane compartments for regulated release and uptake, lipids are free to diffuse across cell bilayers, and, therefore, their signaling capacity is primarily controlled by a dynamic balance between enzymatic biosynthesis and degradation. In the nervous system, FAAs appear to be produced from phospholipid precursors by a calcium-stimulated two-step enzymatic pathway [10, 11]. The inactivation of these lipids is predominantly mediated by enzymatic hydrolysis, a process in which the integral membrane protein fatty acid amide hydrolase (FAAH) plays a primary role [12].

FAAH^{−/−} mice possess highly elevated levels of FAAs throughout the central nervous system (CNS) and some peripheral tissues [5, 13], a metabolic phenotype that correlates with a cannabinoid receptor 1 (CB1)-dependent reduction in pain sensation in these animals [14]. FAAH^{−/−} mice also exhibit reduced inflammation in multiple peripheral models [13, 15], although this phenotype may be mediated, at least in part, by noncannabinoid FAAs [13]. Other than these specific alterations, FAAH^{−/−} animals appear normal [5], suggesting that this enzyme could represent an attractive therapeutic target for pain, inflammation, and possibly other neural disorders [16, 17]. Consistent with this premise, multiple classes of FAAH inhibitors have been generated and have been shown to produce CB1-dependent analgesic [18, 19] and anxiolytic [20] effects in rodents.

FAAH is a member of an unusual class of serine hydrolases termed the amidase signature family, and it utilizes a serine-serine-lysine catalytic triad [21, 22]. Despite its atypical catalytic mechanism, FAAH is susceptible to inhibition by most classical serine hydrolase-directed inhibitors, including fluorophosphonates (FPs) [23], trifluoromethyl ketones [24, 25], α -keto heterocycles [26], and carbamates [20]. This fourth class of FAAH inhibitors is particularly efficacious in vivo, possibly due to its proposed irreversible mechanism of action, analogous to the inactivation of acetylcholinesterase by commercial carbamate drugs (e.g., pyridostigmine, rivastigmine) for the treatment of Alzheimer's disease [27]. The lead carbamate FAAH inhibitors URB532 and URB597 (Table 1) have been modeled into the FAAH active site, with initial results suggesting that their biphenyl substituents mimic the arachidonoyl chain of the FAAH substrate anandamide [28]. However, no experimental data on the mechanism of carbamate inhibition of FAAH have yet been reported. Here, we provide direct evidence that carbamates inactivate FAAH through a mechanism that involves covalent carbamylation of the enzyme's serine nucleophile S241. Interestingly, these results suggest that URB532 and URB597 bind to the FAAH active site in an orientation opposite of that predicted from original modeling studies. Based on these experimental data, we designed: (1) a set of FAAH inhibitors with improved potency, and (2) an active site-directed “click” chemistry (CC) probe for functional analysis of FAAH activity and inhibition in vivo. The CC probe was used to profile the target selectivity of FAAH-directed carbamates in vivo, providing a global view of proteomic “hot spots” for off-target activity of these inhibitors.

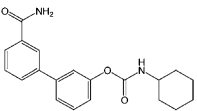
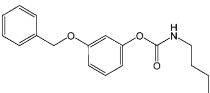
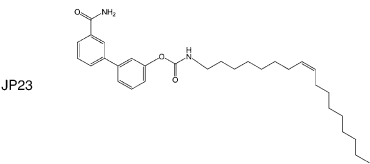
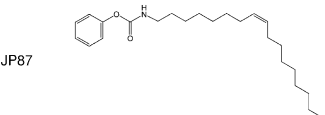
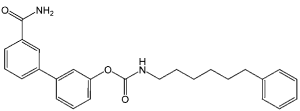
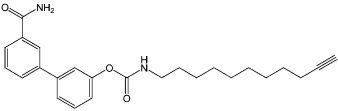
Results

Characterization of the Mechanism of FAAH Inhibition by Carbamates

Several carbamate inhibitors of FAAH have been described in both the scientific [20] and patent [29] literature. The provocative behavioral effects of these agents, including reductions in pain sensation [19, 29] and anxiety [20], have provided support for FAAH as a potential therapeutic target. Nonetheless, the mechanism

*Correspondence: cravatt@scripps.edu

Table 1. Inhibitory Activity of FAAH-Directed Carbamates

Name	Structure	Radioactive Substrate IC ₅₀ (nM)	ABPP IC ₅₀ (nM)
URB597		48 (41–57)	45 (31–65)
URB532		350 (215–570)	410 (260–660)
JP23		58 (32–110)	17 (13–23)
JP87		190 (95–400)	400 (290–540)
JP83		14 (10–18)	1.6 (1.2–2.2)
JP104		7.3 (5.6–9.6)	1.6 (1.2–2.1)

IC₅₀ values (nM [95% confidence limits]) for FAAH carbamate inhibitors determined with purified recombinant enzyme by using a radiolabeled substrate (¹⁴C-oleamide) assay [45] or with unsolubilized mouse brain membranes by competitive ABPP [39].

by which carbamates inhibit FAAH remains obscure, thus complicating efforts to rationally design second-generation agents with superior potency and selectivity. Carbamates typically inhibit serine hydrolases by an irreversible (or slowly reversible) mechanism involving carbamylation of the serine nucleophile [30]. Initial modeling studies with the carbamates URB597 and URB532 suggested that their *O*-biaryl substituents reside in the acyl chain binding (ACB) channel of FAAH, serving as a more rigid structural mimetic of the arachidonoyl chain of the FAAH substrate anandamide [28] (Figure 1A). However, this orientation of binding would place the *N*-alkyl substituents of carbamates in the cytoplasmic access (CA) channel of FAAH in positions more suitable for serving as leaving groups (akin to the ethanolamine of anandamide), possibly resulting in carbonylation of the enzyme's nucleophile (Figure 2A). More recent chemical reactivity studies have raised questions about this model, as the extent of electrospray ionization-induced cleavage of the C(O)-O bond in a series of FAAH

carbamate inhibitors was found to correlate with their potency of inhibition [31], suggesting that *O*-aryl esters may serve as leaving groups in FAAH-carbamate reactions (carbamylation, Figure 2A). Finally, both of the aforementioned models assume that carbamates inhibit FAAH through a covalent mechanism of action, a premise that has not yet been directly tested.

To examine the mechanism of carbamate inhibition of FAAH, purified recombinant enzyme was treated with URB532 or URB597 for 1 hr, after which the protein samples were subjected to tryptic digestion and MALDI-TOF mass spectrometry (MS) analysis. In each case, a new mass signal was observed for the inhibitor-treated sample compared to untreated FAAH controls that corresponded to the mass of the FAAH tryptic peptide amino acids (AA) 217–243, which contain the FAAH nucleophile S241 [32], modified by the C(O)-*N*-alkyl substituent of the inhibitor (Figures 2B–2D). No evidence of C(O)-*O* aryl modification of FAAH was detected in either the URB532 or URB597 reaction. Liquid

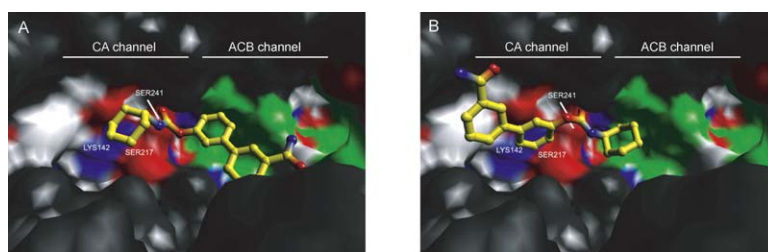


Figure 1. Two Possible Binding Modes for O-Biaryl Carbamate Inhibitors of FAAH

(A and B) The carbamate inhibitor URB597 was modeled into the FAAH active site in two different orientations. In (A), the O-biaryl group of URB597 is located in the acyl chain binding (ACB) channel of FAAH and mimics the location of the arachidonyl chain of FAAH substrates/inhibitors [21]. In (B), the O-biaryl group of URB597 is located in the cytoplasmic access (CA) channel of FAAH, positioning the phenolic oxygen near the S217-K142 residues of the catalytic triad (S241-S217-K142) responsible for leaving group protonation. Blue, basic; red, acidic; green, hydrophobic (see [21] for more details on FAAH crystal structure).

chromatography-tandem electrospray MS (LC-MS) analysis assigned the specific site of carbamylation to S241 with high confidence ($X_{\text{corr}} = 6.04$; $\Delta \text{CN} = 0.54$).

These MS results indicated that URB532 and URB597 inhibit FAAH by carbamylation of the enzyme's serine nucleophile. As a corollary, the O-biaryl substituents

of these agents would be expected to reside in the CA (rather than the ACB) channel of the FAAH active site, where they would be susceptible to enzyme-catalyzed protonation to enhance their function as leaving groups [21, 33] (Figure 1B). To further test this prediction, we synthesized a series of URB597 derivatives in which

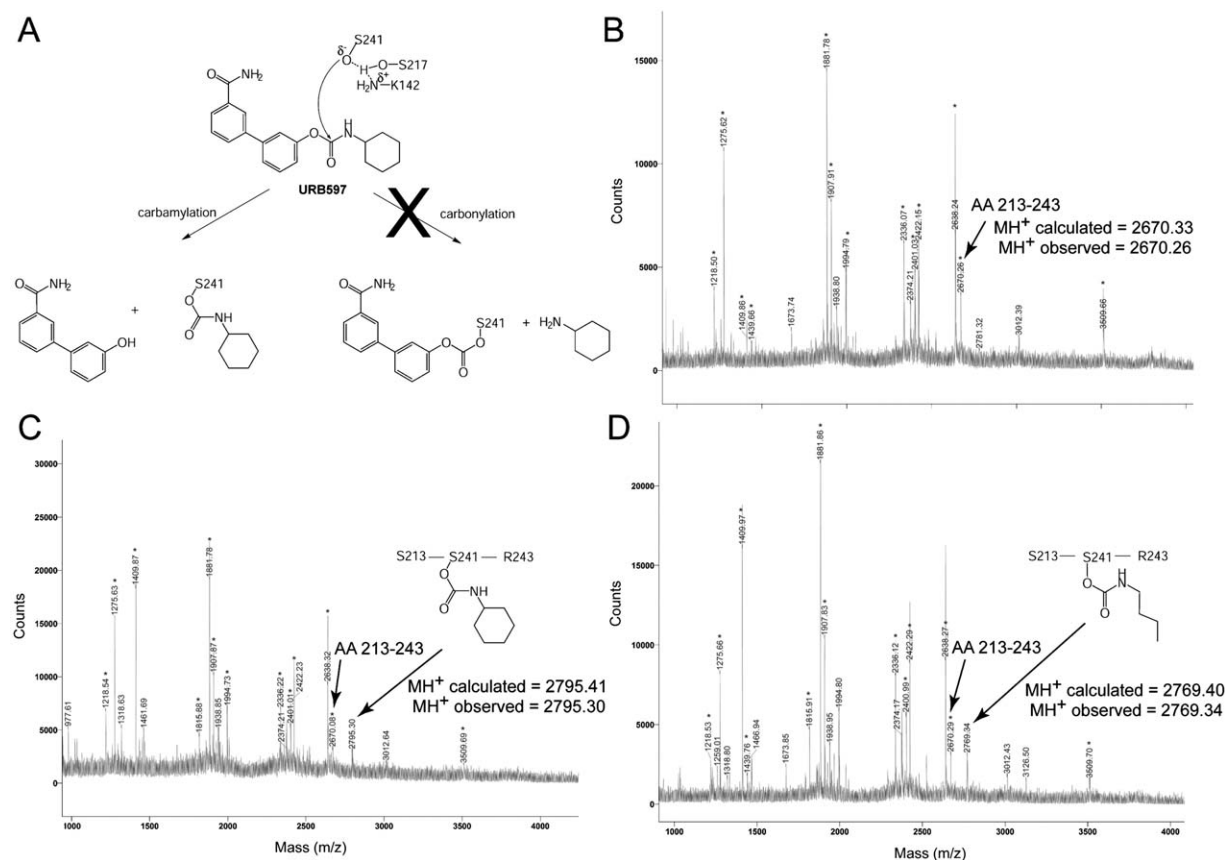


Figure 2. Evidence that URB532 and URB597 Covalently Inhibit FAAH by Carbamylation of the Enzyme's S241 Nucleophile

(A) Two possible modes for covalent labeling of FAAH by URB597. In the left scheme, the O-biaryl group of URB597 serves a leaving group, resulting in carbamylation of the enzyme. In the right scheme, the N-cyclohexyl group of URB597 serves a leaving group, resulting in carbonylation of the enzyme.

(B–D) The MS data shown support the left scheme. (B) MALDI-MS mapping of a tryptic digest of purified recombinant FAAH, highlighting the tryptic peptide that contains the FAAH nucleophile S241 (AA213-243). (C and D) MALDI-MS mapping of a tryptic digest of FAAH pretreated with (C) URB597 and (D) URB532, highlighting new tryptic peptides with masses that correspond to the AA213-243 peptide modified by one molecule of C(O)NH-cyclohexane and C(O)NH-butane, respectively. Asterisked peptides correspond to other FAAH tryptic peptides.

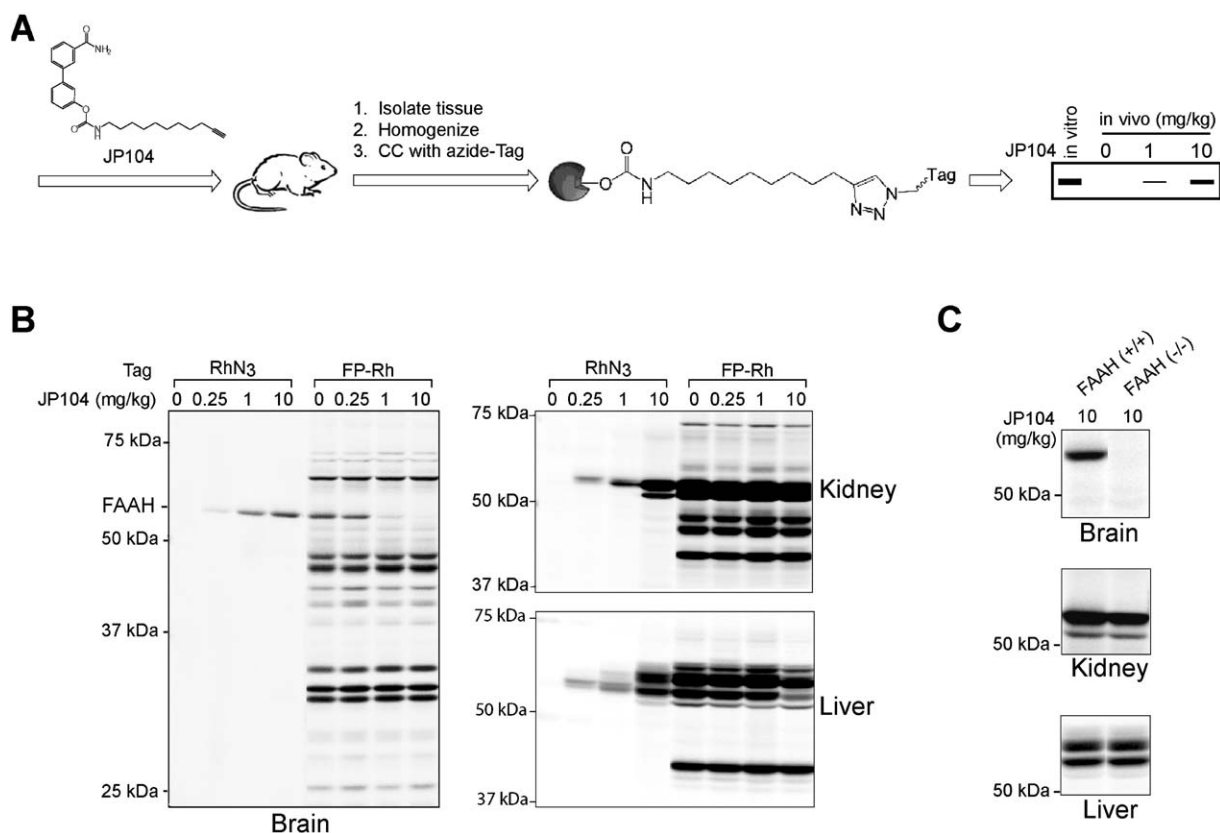


Figure 3. In Vivo Proteomic Profiling of Carbamate Targets with the CC Probe JP104

(A) General method for characterizing the proteome reactivity of JP104 in vivo. Mice are administered JP104 at escalating doses (e.g., 0.25–10 mg/kg, i.p.). After 1 hr, the animals are sacrificed, and their tissues are removed, homogenized, and reacted under CC conditions with an azide-modified rhodamine reporter tag (RhN₃). Labeled proteins are visualized by in-gel fluorescence scanning.

(B and C) Membrane protein reactivity profiles of JP104 in various mouse tissues. A single 65 kDa JP104 target was identified in brain (RhN₃ lanes). (C) This protein was confirmed as FAAH based on its absence in FAAH^{-/-} brains (upper panel). The selective labeling of FAAH by JP104 in brain tissue was further supported by competitive ABPP experiments with the serine hydrolase-directed probe FP-rhodamine (FP-Rh), which showed that none of the other brain serine hydrolases reacted with JP104 (FP-Rh lanes). (B) Additional targets of JP104 were identified in liver and kidney (right panels, RhN₃ lanes). (C) These proteins represented neither FAAH nor FAAH isoforms, as their labeling persisted in FAAH^{-/-} tissues (middle and lower panels). Similar profiles were observed in soluble fractions of mouse kidney and liver (see Figure S2). Fluorescence images are shown in grayscale.

the *N*-cyclohexyl substituent was replaced with various *N*-alkyl groups that mimicked the structures of acyl chains of known FAAH substrates/inhibitors. These carbamates, which included *N*-oleyl (JP23) and *N*-(6-phenyl)hexyl (JP83) analogs, were found to inhibit FAAH with equal or greater potency than URB597 (Table 1). These data indicate that the URB597 *O*-biaryl substituent can be accommodated in the CA channel of the FAAH active site. Indeed, it appears that this group displays positive binding interactions with the CA channel, as its replacement with a phenyl moiety (JP87) significantly reduced inhibitor potency (Table 1).

Generation of a Click Chemistry Probe to Evaluate the Proteome-Wide Reactivity of FAAH-Directed Carbamates In Vivo

Covalent inhibitors, such as carbamates, are generally regarded with skepticism as potential drugs due to their inherent reactivity [34], which is perceived to compromise target selectivity in vivo. Nonetheless, this assertion often goes untested, as general methods to

determine the in vivo target selectivity of covalent inhibitors are lacking. The discovery that URB597 inhibited FAAH via covalent carbamylation of the enzyme's active site inspired us to synthesize an *N*-alkynyl derivative of this agent, JP104, which we hypothesized could be used to directly identify the targets of FAAH-directed carbamates in vivo. In this approach, tissues from animals treated with JP104 are reacted with a complementary azide-modified reporter tag (e.g., azido-rhodamine [RhN₃], azido-biotin [35, 36]) under CC conditions to afford the corresponding triazole products (Figure 3A). Initial in vitro experiments revealed that JP104 was a potent FAAH inhibitor in vitro (Table 1) and selectively labeled this enzyme in brain membrane extracts (Figure S1A; see the Supplemental Data available with this article online). To further confirm the specificity of JP104 for FAAH, we treated the JP104-labeled brain proteome with a rhodamine-tagged fluorophosphonate (FP-Rh), which serves as a general activity-based protein profiling (ABPP) probe for the serine hydrolase superfamily [37–39]. JP104 completely blocked FP-Rh labeling of

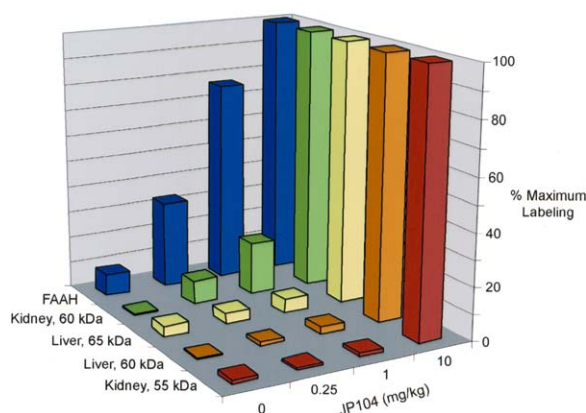


Figure 4. Dose Dependence of Protein Labeling by JP104 In Vivo. At 1 mg/kg JP104 (i.p.), the labeling of FAAH was approximately 80% of maximum, while none of the off-target sites were labeled at greater than 20% of maximum. Data represent the average of three trials per dose of JP104.

FAAH at 100 nM, but it did not inhibit the labeling of any other brain serine hydrolases at concentrations up to 10 μ M (Figure S1B).

We next tested whether click chemistry (CC) methods could be used to identify the targets of JP104 in vivo. Mice were treated with JP104 (10 mg/kg, intraperitoneal [i.p.]) for 1 hr, after which they were sacrificed and their tissues removed for CC analysis. Consistent with in vitro studies, FAAH was the primary in vivo target of JP104 observed in brain tissue (Figure 3B, left panel). In contrast, several additional targets of JP104, including multiple membrane-associated liver and kidney proteins, were detected in peripheral tissues (Figure 3B, right panels). These JP104-labeled proteins were also observed in in vivo-labeled, soluble proteomes from kidney and liver (Figure S2), as well as in FAAH^{-/-} tissues (Figure 3C), indicating that they do not represent FAAH or potential FAAH isoforms. Dose-response profiles identified a concentration range for JP104 (0.25–1.0 mg/kg) over which significant FAAH inhibition could be achieved without extensive modification of additional targets (Figure 4). For example, at 1 mg/kg JP104, FAAH labeling was ~80% of maximum in the brain, whereas none of the liver and kidney targets were modified to greater than 20%. The nearly complete inactivation of brain FAAH in vivo by 1 mg/kg JP104 was confirmed by competitive ABPP studies with FP-Rh (Figure 3B, left panel). In contrast, JP104 did not significantly reduce the intensity of FP-Rh signals in liver and kidney proteomes (Figure 3B, right panels), which likely reflects the presence of several comigrating serine hydrolase activities in the 60–65 kDa range in these tissues (only a subset of which are modified by JP104). These results indicate that carbamate-based inhibitors can be designed that selectively target FAAH in vivo, albeit over a somewhat limited concentration range.

Identification and Characterization of In Vivo Targets of JP104

The molecular characterization of off-target sites of reactivity for FAAH-directed carbamates would greatly assist medicinal chemistry efforts aimed at improving

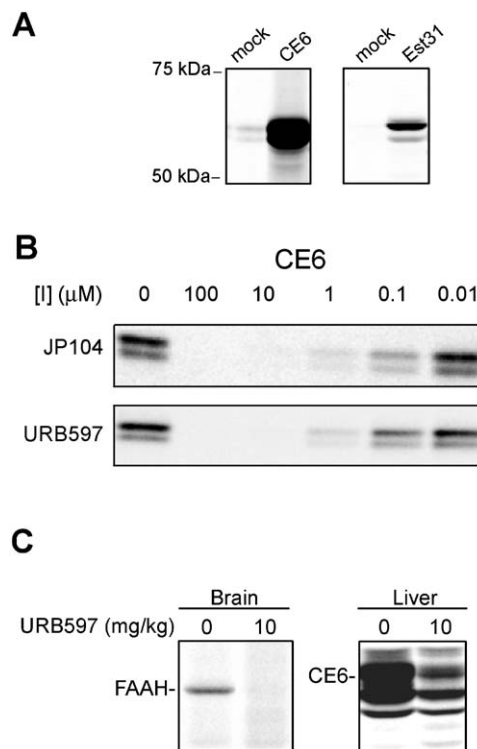


Figure 5. Characterization of In Vivo Off-Target Sites of FAAH-Directed Carbamates

(A) Labeling of recombinant CE6 and Est31 in transfected COS7 cell proteomes by JP104 (1 μ M).

(B) Inhibition of FP-Rh labeling of recombinant CE6 by JP104 and URB597 (100 nM FP-Rh, 0.01–100 μ M JP104 and URB597). From these data sets, IC₅₀ values of approximately 50 and 200 nM were estimated for JP104 and URB597, respectively (see Table S1 for complete data on CE6 inhibition). I, inhibitor.

(C) Inhibition of FAAH and CE6 by URB597 in vivo. Administration of URB597 to mice (10 mg/kg, i.p., 1 hr) blocked JP104 labeling of brain FAAH (left panel) and the 60–65 kDa liver target identified as CE6 (right panel). JP104 labeling was conducted in vitro by using membrane proteomes of tissues from URB597-treated mice and was visualized by CC with RhN₃. Equivalent inhibition of JP104 labeling of CE6 was observed in liver soluble proteomes from URB597-treated mice (data not shown). Fluorescence images are shown in grayscale.

the selectivity of these agents. With this goal in mind, we reacted liver cytoplasmic proteomes from JP104-treated mice (10 mg/kg, i.p.) with an azide-modified biotin tag under CC conditions. Biotinylated proteins were then enriched by avidin chromatography, separated by SDS-PAGE, and subjected to trypsin digestion and LC-MS analysis. In the mass range of 60–65 kDa, two candidate targets of JP104—carboxylesterase 6 (CE6) and esterase 31 (Est31)—were identified. These enzymes were confirmed as specific targets of JP104 by recombinant expression in COS7 cells (Figure 5A). Using competitive ABPP [39], in which transfected COS7 cell proteomes were first pretreated with varying concentrations of JP104 (0.01–10 μ M) and then incubated with FP-Rh (100 nM), we estimated IC₅₀ values of 0.05 and 2 μ M for CE6 and Est31, respectively (Figure 5B and Table S1). CE6 was also inhibited by URB597 with similar potency (IC₅₀ = 0.2 μ M, Figure 5B), while Est31 was not labeled by this carbamate in vitro (Table S1). To test

whether CE6 was targeted by URB597 in vivo, mice were treated with this inhibitor (10 mg/kg, i.p.) for 1 hr, and the JP104-labeling profiles of excised tissues were compared to those of vehicle-treated animals. In addition to blocking JP104 labeling of FAAH in brain, URB597 significantly reduced the labeling of the 60–65 kDa CE6/Est31 bands in liver (Figure 5C). Given that only CE6 is sensitive to inhibition by URB597 in vitro, we speculate that the labeling signals observed for the 60–65 kDa bands in vivo are predominantly derived from this enzyme. Finally, dose-response studies with URB597 revealed that this inhibitor and JP104 displayed similar efficacies for inhibiting FAAH (Figure S3), indicating that URB597 also shows a moderate (5- to 10-fold) range of selectivity for this enzyme over CE6 in vivo.

Discussion

Nearly 30% of the enzymes targeted by drugs in clinical use today are inhibited by a covalent irreversible mechanism [40]. This surprisingly large percentage suggests that prejudices against the development of irreversible inhibitors as therapeutic agents are overstated. The primary concern with covalent agents is that their inherent reactivity will result in a lack of target selectivity in vivo, although this presumption is rarely tested in a comprehensive way. Here, we describe a general strategy to map the proteome-wide reactivity of covalent inhibitors in vivo. This approach, which was used to evaluate the selectivity of carbamate inhibitors of the endocannabinoid-degrading enzyme FAAH, exploits the bioorthogonal CC reaction to modify inhibitor-labeled enzymes with reporter tags for their direct visualization, enrichment, and identification [35, 36]. Notably, the success of this CC strategy hinged on a detailed understanding of the mechanism of carbamate inhibition of FAAH, such that an alkyne could be appended to the segment of the inhibitor (the *N*-alkyl group) that remained bound to the FAAH active site.

Using an alkyne-derivatized carbamate (JP104), we identified multiple enzymes inactivated by FAAH-directed carbamates in vivo, including both known (Est31) and uncharacterized (CE6) proteins. It is perhaps not surprising that these off-targets of JP104 are, like FAAH, serine hydrolases, given that carbamates show a preferred reactivity with enzymes from this class. Nonetheless, it is important to emphasize that the approach described herein is not limited, like previously described ABPP methods [39, 41], to profiling small-molecule targets within a given enzyme class, but rather can identify any protein susceptible to covalent inactivation by chemical probes. Moreover, because CC methods can be applied to study small-molecule-protein interactions in vivo, they take into account several key factors, such as compound biodistribution and metabolism, as well as the dynamic regulation of enzyme localization and activity, that are not effectively addressed with in vitro methods.

By integrating information on the in vivo efficacy and selectivity of JP104, a dose range was identified over which FAAH could be inhibited without extensive labeling of other enzymes. The comparison of in vivo reactivity profiles at several doses of probe was critical for

establishing the extent of labeling of individual proteins and normalizing for differences in relative enzyme abundance. For example, at 1.0 mg/kg JP104, stronger absolute signal intensities were observed for off-targets in the liver and kidney than for FAAH in the brain (Figure 3B). However, administration of higher doses of JP104 (10 mg/kg) revealed that only a modest fraction of these off-targets was labeled at lower doses, while FAAH labeling was nearly complete at 1 mg/kg probe (Figures 3B and 4). These results suggest that the liver and kidney off-targets likely represent more abundant, but less potently inhibited, targets of JP104 than FAAH, a premise that is also supported by in vitro IC_{50} calculations (JP104 inhibited FAAH and CE6 with IC_{50} values of approximately 2 and 50 nM, respectively). Thus, these studies appear to have defined an acceptable pharmacological window for the administration of FAAH inhibitors in vivo, at least for basic research purposes in mice. The application of FAAH inhibitors in clinical settings may require a greater selectivity index than is afforded by current compounds. Future medicinal chemistry efforts aimed at optimizing the specificity of FAAH-directed carbamates should be assisted by the identification of enzymes like CE6 that represent general “hot spots” of reactivity for these compounds in vivo. In this regard, it is worth noting that neither CE6 nor Est31 share any sequence similarity with FAAH, thus reinforcing the notion that sequence-unrelated enzymes can share significant active site homology [18, 39] and highlighting the importance of unbiased approaches for the evaluation of inhibitor selectivity in vivo.

Some potential limitations of the CC approach should also be noted. First, in situ proteome reactivity data sets are currently analyzed by one-dimensional gel electrophoresis, which has limited resolving power and therefore may fail to identify certain lower-abundance targets that comigrate with more highly expressed proteins. For example, while the labeling of FAAH by JP104 could be visualized in brain, this enzyme was not detectable in liver and kidney proteomes due to comigrating targets, even though these tissues are known to express FAAH. Recent advances in gel-free (LC-MS-based) approaches for chemical proteomics should address this issue [42, 43]. A second concern relates to how chemical derivatization might affect the proteome reactivity profile of covalent drugs. Though the addition of an alkyne group to the structures of most small molecules should be feasible with minimal steric perturbation, this modification could still, in certain cases, alter a compound's binding and/or reactivity. This issue can at least be partially addressed by in vivo competition studies, in which the parent inhibitor is used to block the labeling of probe targets, as was carried out with the URB597/JP104 small-molecule/probe pair (Figure 5C). In such assays, “false positive” signals (i.e., proteins that selectively react with the probe) would be detected as targets whose labeling is not competed by excess inhibitor. “False negative” signals (i.e., proteins that selectively react with the parent inhibitor) might be revealed by constructing multiple probes in which the alkyne is incorporated at different locations on the parent inhibitor structure.

The in vivo profiling methods described herein should be applicable to any compound that operates through

a covalent mechanism of action. While irreversible inhibitors are often viewed unfavorably as potential therapeutic agents [34], they do possess some advantages over reversible compounds. For example, as has been previously noted [44], irreversible inhibitors typically lead to the complete and long-lasting inactivation of target proteins, thus generating maximal pharmacological effects from a single administration. In addition, because covalent compounds can inactivate enzymes at concentrations far below their respective binding constants, low quantities of drug are required in vivo, and nonspecific interactions that would otherwise occur at high compound levels may be avoided. These observations, coupled with the advent of general methods to directly identify the proteins labeled by reactive small molecules in vivo, suggest, perhaps somewhat counterintuitively, that it may be easier to comprehensively assess and optimize the selectivity of irreversible inhibitors compared to reversible agents. The success of such integrated functional proteomic and medicinal chemistry endeavors has the potential to reshape our views on the suitability of covalent small molecules as pharmacological agents for basic research and clinical applications.

Significance

Fatty acid amide hydrolase (FAAH) terminates the signaling function of a large and diverse class of endogenous signaling lipids referred to as fatty acid amides. Carbamate inhibitors of FAAH have been reported to show analgesic and anxiolytic properties in rodents. However, the mechanism by which carbamates inhibit FAAH has remained obscure, thus complicating the rational design of agents with improved potency and selectivity. Here, we provide direct biochemical evidence that carbamates covalently modify the active site of FAAH and use this information to design a series of inhibitors that display enhanced potency. One of these carbamates was converted into a “click chemistry” probe for in vivo analysis of FAAH activity and inhibition. This activity-based probe was used to comprehensively assess the proteome reactivity of FAAH-directed carbamate inhibitors in vivo, revealing that these agents are selective for FAAH in the nervous system but react with several other enzymes in peripheral tissues. In vivo dose-response curves identified a modest window of selectivity (~5- to 10-fold) across which carbamates could inhibit FAAH without extensive labeling of off-target enzymes. The general experimental strategy presented herein can be applied to create in vivo functional probes for any enzyme susceptible to covalent inhibition. Considering that nearly 30% of the enzymes targeted by drugs in current clinical use are inhibited by an irreversible mechanism, we anticipate that click chemistry probes should play a major role in the future development of enzyme inhibitors for both basic research and clinical applications.

Experimental Procedures

Synthesis of Inhibitors
See Supplemental Data.

MS Analysis of Carbamate Labeling Site of FAAH

Inhibitor labeling reactions were conducted at room temperature with 10 μ M recombinant purified FAAH (~30 μ g) prepared as described previously [45] and 200 μ M URB597 or URB532 in 125 mM Tris·HCl (pH 9.0), 0.01% Triton X-100 in a total volume of 50 μ l. Any noncovalent interactions between probe and enzyme were disrupted by gel filtration through a Biorad 10DG column, and the desired fractions were concentrated to 50 μ l by using an Amicon Ultra centrifugal filter device, MWCO 10,000. Samples were then denatured in 8 M urea and subjected to reduction, alkylation, and tryptic digestion according to established procedures [46]. Samples (50 μ l after concentration under reduced pressure) were desalted by C₁₈ ZipTip (Millipore) eluting in 4 μ l (3:1 acetonitrile/water with 0.1% trifluoroacetic acid) and were analyzed by MALDI-TOF Reflectron mass spectrometry (Applied Biosystems Voyager STR) with 1:1 matrix α -cyano-4-hydroxycinnamic acid:sample (1 μ l total volume). For tandem MS analysis, recombinant purified FAAH (~30 μ g) in 125 mM Tris·HCl (pH 9) was reacted with URB597 as described above and was then directly subjected to the tryptic digestion protocol. The resulting peptide mixture (50 μ l after concentration under reduced pressure) was analyzed by reverse-phase liquid chromatography-electrospray ionization tandem MS (Finnigan LCQ Deca ion trap MS; Thermo Finnigan). The gradient elution began with 100% buffer A (95:5 vol/vol water/acetonitrile containing 0.1% formic acid) for 10 min, followed by an increase to 15% buffer B (80:20 vol/vol acetonitrile/water containing 0.1% formic acid) in 5 min. The gradient increased linearly to 50% buffer B in 75 min, followed by an increase to 100% buffer B in 10 min, and ending with 100% buffer B for 10 min. Tandem mass spectra were searched against a database containing the rat FAAH sequence by using a modified version of the SEQUEST algorithm. Search results were filtered and grouped with DTASelect [47].

Preparation of Mouse Tissue Proteomes for CC Analysis

Mouse tissues were Dounce-homogenized in 10 mM sodium/potassium phosphate buffer (pH 8.0) (PB), followed by a low-speed spin (890 \times g) to remove debris. The supernatant was then subjected to centrifugation at 100,000 \times g for 45 min to provide the cytosolic fraction in the supernatant and the membrane fraction as a pellet, which was washed and resuspended in PB buffer by sonication. The total protein concentration in each fraction was determined by a protein assay kit (Bio-Rad). Samples were stored at -80°C until use.

In Vitro Analysis of Inhibitor Potency

Inhibitor analysis was carried out in vitro by using two different assays. First, a radioactive substrate assay was employed by using purified, recombinant FAAH as described previously [32, 45]. Briefly, FAAH activity was determined in the presence of varying concentrations of inhibitors (0.01–100 μ M, 50 \times DMSO stocks) by following the conversion of [¹⁴C]oleamide to oleic acid by thin-layer chromatography. Inhibitor potency was also examined by using competitive ABPP as described previously [39]. Briefly, membrane proteomes of mouse tissues were diluted to 1 mg/ml and preincubated with varying concentrations of inhibitors (10 nM–100 μ M, 50 \times DMSO stocks) for 10 min at room temperature prior to the addition of a rhodamine-tagged fluorophosphonate (FP-Rh; [38]) ABPP probe at a final concentration of 100 nM in a 50 μ l total reaction volume. Reactions were quenched after 10 min with one volume 2 \times SDS loading buffer (reducing with protease inhibitor), run on SDS-PAGE, and visualized with a flatbed fluorescence scanner. Dose-response curves obtained from both methods from three trials at each inhibitor concentration were fit with Prism software (GraphPad) to obtain IC₅₀ values with 95% confidence intervals.

In Vitro CC Analysis of Proteins with JP104

Proteome samples (43 μ l of 1 mg/ml protein in PB) were treated with 100 nM JP104 (unless otherwise indicated) (1 μ l of a 5 μ M DMSO stock) for 1 hr at room temperature, followed by CC reaction with 25 μ M rhodamine-azide (RhN₃, 1 μ l of a 1.25 mM DMSO stock) as previously described [35, 36]. Samples were analyzed separately by competitive ABPP with 1 μ M FP-Rh instead of the CC reaction with RhN₃. Reactions were quenched with an equal volume (50 μ l) of 2 \times SDS loading buffer (reducing with protease inhibitor), run on SDS-PAGE, and visualized by in-gel fluorescence scanning with a

Hitachi FMBio Ile flatbed laser-induced fluorescence scanner (MiraiBio, Alameda, CA).

In Vivo Labeling in Mice

Mice (male C57BL/6 or FAAH^{-/-} [5]), weighed between 20 and 30 g and were between the ages of 12 and 18 weeks. Mice were given intraperitoneal (i.p.) injections of JP104 (0, 0.25, 1, and 10 mg/kg) or URB597 (0, 0.1, 0.2, 1, and 10 mg/kg) in vehicle (18:1:1 saline:emulphor:EtOH). The mock injections (0 mg/kg) consisted solely of vehicle. After 1 hr, the mice were sacrificed by CO₂ asphyxiation and decapitation, and relevant tissues were flash frozen (with liquid N₂) immediately upon removal. Tissues were processed as described above to isolate membrane and cytosolic proteomes. The CC reaction and/or FP-Rh labeling were carried out as described above, and reactions were analyzed by SDS-PAGE. The average of three independent samples at each concentration was reported.

Protein Isolation and Identification from Mouse Liver

To identify off-target sites of reactivity in the liver, trifunctional probes with biotin, Rh, and an azide [36] were used to affinity purify in vivo-labeled enzymes for identification by mass spectrometry techniques. The soluble liver proteome (2.5 ml, 3 mg/ml protein) from a mouse treated with JP104 (10 mg/kg, i.p.) was subjected to PD-10 size-exclusion chromatography to remove excess probe and was then fractionated by Q-Sepharose chromatography (0–2 M NaCl gradient). Fractions containing desired material were combined, and a 480 μ l aliquot was subjected to CC reaction with the trifunctional azide probe. The excess CC reagents were removed in a series of washes as previously described [36]. Tagged proteins were enriched by using avidin-agarose beads, and the affinity-isolated proteins were separated by SDS-PAGE as previously described [36]. Gel bands were identified by in-gel fluorescence scanning, excised, and subject to in-gel trypsin digest [36]. The resulting peptides were analyzed by μ LC-MS/MS, and the results were searched against public databases by using SEQUEST to identify probe-labeled proteins as carboxylesterase 6 (CE6; GI# 20071857) and esterase 31 (Est31; GI# 2494382). These off-target proteins were further verified by purchasing expressed sequence tags (Open Biosystems), sequencing, and transient transfection into COS7 cells as described previously [39]. Cytosolic fractions from transfected cells were isolated by centrifugation and were analyzed in vitro as described above to confirm labeling with JP104. IC₅₀ values were determined via competitive ABPP as described previously [39].

Supplemental Data

Supplemental Data including synthesis of inhibitors and probes and figures showing additional proteome labeling results and a comparison of JP104 and URB597 dose-response profiles are available at <http://www.chembiol.com/cgi/content/full/12/11/1179/DC1/>.

Acknowledgments

We thank M. Bracey for assistance with Figure 1, A. Speers for assistance with CC protocols and reagents, S. Niessen for assistance with tandem MS analysis, B. Webb for assistance with MALDI-MS analysis, K. Chiang for assistance with the in vivo mouse studies, A. Saghatelian for samples of URB597 and URB532, and the Cravatt lab for helpful discussions and critical reading of the manuscript. This work was supported by the National Institutes of Health (DA017259 and DA015197 to B.F.C. and DA019347 to J.P.A.), the Helen L. Dorris Child and Adolescent Neuro-Psychiatric Disorder Institute, and the Skaggs Institute for Chemical Biology.

Received: August 2, 2005

Accepted: August 18, 2005

Published: November 18, 2005

References

- Bos, C.L., Richel, D.J., Ritsema, T., Peppelenbosch, M.P., and Versteeg, H.H. (2004). Prostanoids and prostanoid receptors in signal transduction. *Int. J. Biochem. Cell Biol.* 36, 1187–1205.
- Fukushima, N., Ishii, I., Contos, J.J., Weiner, J.A., and Chun, J. (2001). Lysophospholipid receptors. *Annu. Rev. Pharmacol. Toxicol.* 41, 507–534.
- Maccarrone, M., and Finazzi-Agro, A. (2002). Endocannabinoids and their actions. *Vitam. Horm.* 65, 225–255.
- Fowler, C.J., Holt, S., Nilsson, O., Jonsson, K.O., Tiger, G., and Jacobsson, S.O. (2005). The endocannabinoid signaling system: pharmacological and therapeutic aspects. *Pharmacol. Biochem. Behav.* 81, 248–262.
- Cravatt, B.F., Demarest, K., Patricelli, M.P., Bracey, M.H., Giang, D.K., Martin, B.R., and Lichtman, A.H. (2001). Supersensitivity to anandamide and enhanced endogenous cannabinoid signaling in mice lacking fatty acid amide hydrolase. *Proc. Natl. Acad. Sci. USA* 98, 9371–9376.
- Rodriguez de Fonseca, F., Navarro, M., Gomez, R., Escuredo, L., Nava, F., Fu, J., Murillo-Rodriguez, E., Giuffrida, A., LoVerme, J., Gaetani, S., et al. (2001). An anorexic lipid mediator regulated by feeding. *Nature* 414, 209–212.
- Cravatt, B.F., Prospero-Garcia, O., Siuzdak, G., Gilula, N.B., Henriksen, S.J., Boger, D.L., and Lerner, R.A. (1995). Chemical characterization of a family of brain lipids that induce sleep. *Science* 268, 1506–1509.
- Devane, W.A., Hanus, L., Breuer, A., Pertwee, R.G., Stevenson, L.A., Griffin, G., Gibson, D., Mandelbaum, A., Etinger, A., and Mechoulam, R. (1992). Isolation and structure of a brain constituent that binds to the cannabinoid receptor. *Science* 258, 1946–1949.
- Lambert, D.M., Vandevoorde, S., Jonsson, K.O., and Fowler, C.J. (2002). The palmitoylethanolamide family: a new class of anti-inflammatory agents? *Curr. Med. Chem.* 9, 663–674.
- Cadas, H., Gaillat, S., Beltramo, M., Venance, L., and Piomelli, D. (1996). Biosynthesis of an endogenous cannabinoid precursor in neurons and its control by calcium and cAMP. *J. Neurosci.* 16, 3934–3942.
- Cadas, H., di Tomaso, E., and Piomelli, D. (1997). Occurrence and biosynthesis of endogenous cannabinoid precursor, N-arachidonyl phosphatidylethanolamine, in rat brain. *J. Neurosci.* 17, 1226–1242.
- Cravatt, B.F., Giang, D.K., Mayfield, S.P., Boger, D.L., Lerner, R.A., and Gilula, N.B. (1996). Molecular characterization of an enzyme that degrades neuromodulatory fatty-acid amides. *Nature* 384, 83–87.
- Cravatt, B.F., Saghatelian, A., Hawkins, E.G., Clement, A.B., Bracey, M.H., and Lichtman, A.H. (2004). Functional disassociation of the central and peripheral fatty acid amide signaling systems. *Proc. Natl. Acad. Sci. USA* 101, 10821–10826.
- Lichtman, A.H., Shelton, C.C., Advani, T., and Cravatt, B.F. (2004). Mice lacking fatty acid amide hydrolase exhibit a cannabinoid receptor-mediated phenotypic hypoalgesia. *Pain* 109, 319–327.
- Massa, F., Marsicano, G., Hermann, H., Cannich, A., Monory, K., Cravatt, B.F., Ferri, G.-L., Sibaev, A., Storr, M., and Lutz, B. (2004). The endogenous cannabinoid system protects against colonic inflammation. *J. Clin. Invest.* 113, 1202–1209.
- Cravatt, B.F., and Lichtman, A.H. (2003). Fatty acid amide hydrolase: an emerging therapeutic target in the endocannabinoid system. *Curr. Opin. Chem. Biol.* 7, 469–475.
- Gaetani, S., Cuomo, V., and Piomelli, D. (2003). Anandamide hydrolysis: a new target for anti-anxiety drugs? *Trends Mol. Med.* 9, 474–478.
- Lichtman, A.H., Leung, D., Shelton, C., Saghatelian, A., Hardouin, C., Boger, D., and Cravatt, B.F. (2004). Reversible inhibitors of fatty acid amide hydrolase that promote analgesia: evidence for an unprecedented combination of potency and selectivity. *J. Pharmacol. Exp. Ther.* 311, 441–448.
- Hohmann, A.G., Suplita, R.L., Bolton, N.M., Neely, M.H., Fegley, D., Mangieri, R., Krey, J.F., Walker, J.M., Holmes, P.V., Crystal, J.D., et al. (2005). An endocannabinoid mechanism for stress-induced analgesia. *Nature* 435, 1108–1112.
- Kathuria, S., Gaetani, S., Fegley, D., Valino, F., Duranti, A., Tonini, A., Mor, M., Tarzia, G., La Rana, G., Calignano, A., et al. (2003). Modulation of anxiety through blockade of anandamide hydrolysis. *Nat. Med.* 9, 76–81.
- Bracey, M.H., Hanson, M.A., Masuda, K.R., Stevens, R.C., and Cravatt, B.F. (2002). Structural adaptations in a membrane

- enzyme that terminates endocannabinoid signaling. *Science* 298, 1793–1796.
22. McKinney, M.K., and Cravatt, B.F. (2005). Structure and function of Fatty Acid amide hydrolase. *Annu. Rev. Biochem.* 74, 411–432.
23. Deutsch, D.G., Omeir, R., Arreaza, G., Salehani, D., Prestwich, G.D., Huang, Z., and Howlett, A. (1997). Methyl arachidonyl fluorophosphonate: a potent irreversible inhibitor of anandamide amidase. *Biochem. Pharmacol.* 53, 255–260.
24. Koutek, B., Prestwich, G.D., Howlett, A.C., Chin, S.A., Salehani, D., Akhavan, N., and Deutsch, D.G. (1994). Inhibitors of arachidonyl ethanolamide hydrolysis. *J. Biol. Chem.* 269, 22937–22940.
25. Boger, D.L., Sato, H., Lerner, A.E., Austin, B.J., Patterson, J.E., Patricelli, M.P., and Cravatt, B.F. (1999). Trifluoromethyl ketone inhibitors of fatty acid amide hydrolase: a probe of structural and conformational features contributing to inhibition. *Bioorg. Med. Chem. Lett.* 9, 265–270.
26. Boger, D.L., Sato, H., Lerner, A.E., Hedrick, M.P., Fecik, R.A., Miyauchi, H., Wilkie, G.D., Austin, B.J., Patricelli, M.P., and Cravatt, B.F. (2000). Exceptionally potent inhibitors of fatty acid amide hydrolase: the enzyme responsible for degradation of endogenous oleamide and anandamide. *Proc. Natl. Acad. Sci. USA* 97, 5044–5049.
27. Ibach, B., and Haen, E. (2004). Acetylcholinesterase inhibition in Alzheimer's Disease. *Curr. Pharm. Des.* 10, 231–251.
28. Mor, M., Rivara, S., Lodola, A., Plazzi, P.V., Tarzia, G., Duranti, A., Tontini, A., Piersanti, G., Kathuria, S., and Piomelli, D. (2004). Cyclohexylcarbamic acid 3'- or 4'-substituted biphenyl-3-yl esters as fatty acid amide hydrolase inhibitors: synthesis, quantitative structure-activity relationships, and molecular modeling studies. *J. Med. Chem.* 47, 4998–5008.
29. Sit, S.-Y., and Xie, K. December 2002. U.S. patent W0 02/087569.
30. Bar-On, P., Millard, C.B., Harel, M., Dvir, H., Enz, A., Sussman, J.L., and Silman, I. (2002). Kinetic and structural studies on the interaction of cholinesterases with the anti-Alzheimer drug rivastigmine. *Biochemistry* 41, 3555–3564.
31. Basso, E., Duranti, A., Mor, M., Piomelli, D., Tontini, A., Tarzia, G., and Traldi, P. (2004). Tandem mass spectrometric data-FAAH inhibitory activity relationships of some carbamic acid O-aryl esters. *J. Mass Spectrom.* 39, 1450–1455.
32. Patricelli, M.P., Lovato, M.A., and Cravatt, B.F. (1999). Chemical and mutagenic investigations of fatty acid amide hydrolase: evidence for a family of serine hydrolase with distinct catalytic properties. *Biochemistry* 38, 9804–9812.
33. McKinney, M.K., and Cravatt, B.F. (2003). Evidence for distinct roles in catalysis for residues of the serine-serine-lysine catalytic triad of fatty acid amide hydrolase. *J. Biol. Chem.* 278, 37393–37399.
34. Sirois, S., Hatzakis, G., Wei, D., Du, Q., and Chou, K.C. (2005). Assessment of chemical libraries for their druggability. *Comput. Biol. Chem.* 29, 55–67.
35. Speers, A.E., Adam, G.C., and Cravatt, B.F. (2003). Activity-based protein profiling in vivo using a copper(I)-catalyzed azide-alkyne [3 + 2] cycloaddition. *J. Am. Chem. Soc.* 125, 4686–4687.
36. Speers, A.E., and Cravatt, B.F. (2004). Profiling enzyme activities in vivo using click chemistry methods. *Chem. Biol.* 11, 535–546.
37. Patricelli, M.P., Giang, D.K., Stamp, L.M., and Burbaum, J.J. (2001). Direct visualization of serine hydrolase activities in complex proteome using fluorescent active site-directed probes. *Proteomics* 1, 1067–1071.
38. Jessani, N., Liu, Y., Humphrey, M., and Cravatt, B.F. (2002). Enzyme activity profiles of the secreted and membrane proteome that depict cancer cell invasiveness. *Proc. Natl. Acad. Sci. USA* 99, 10335–10340.
39. Leung, D., Hardouin, C., Boger, D.L., and Cravatt, B.F. (2003). Discovering potent and selective inhibitors of enzymes in complex proteomes. *Nat. Biotechnol.* 21, 687–691.
40. Robertson, J.G. (2005). Mechanistic basis of enzyme-targeted drugs. *Biochemistry* 44, 5561–5571.
41. Greenbaum, D.C., Arnold, W.D., Lu, F., Hayrapetian, L., Baruch, A., Krumrine, J., Toba, S., Chehade, K., Bromme, D., Kuntz, I.D., et al. (2002). Small molecule affinity fingerprinting. A tool for enzyme family subclassification, target identification, and inhibitor design. *Chem. Biol.* 9, 1085–1094.
42. Okerberg, E.S., Wu, J., Zhang, B., Samii, B., Blackford, K., Winn, D.T., Shreder, K.R., Burbaum, J.J., and Patricelli, M.P. (2005). High-resolution functional proteomics by active-site peptide profiling. *Proc. Natl. Acad. Sci. USA* 102, 4996–5001.
43. Speers, A.E., and Cravatt, B.F. (2005). A tandem orthogonal proteolysis strategy for high-content chemical proteomics. *J. Am. Chem. Soc.* 127, 10018–10019.
44. Fry, D.W., Bridges, A.J., Denny, W.A., Doherty, A., Greis, K.D., Hicks, J.L., Hook, K.E., Keller, P.R., Leopold, W.R., Loo, J.A., et al. (1998). Specific, irreversible inactivation of the epidermal growth factor receptor and erbB2, by a new class of tyrosine kinase inhibitor. *Proc. Natl. Acad. Sci. USA* 95, 12022–12027.
45. Patricelli, M.P., Lashuel, H.A., Giang, D.K., Kelly, J.W., and Cravatt, B.F. (1998). Comparative characterization of a wild type and transmembrane domain-deleted fatty acid amide hydrolase: identification of the transmembrane domain as a site for oligomerization. *Biochemistry* 37, 15177–15187.
46. Patricelli, M.P., and Cravatt, B.F. (2001). Characterization and manipulation of the acyl chain selectivity of fatty acid amide hydrolase. *Biochemistry* 40, 6107–6115.
47. Tabb, D.L., McDonald, W.H., and Yates, J.R., III. (2002). DTASelect and Contrast: tools for assembling and comparing protein identifications from shotgun proteomics. *J. Proteome Res.* 1, 21–26.